Model for the behavior of steel fibers reinforced concrete in plates elements

FERNANDO LOPEZ-GAYARRE*, ALBERTO DOMINGO[a], CARLOS LÁZARO[a],
CARLOS LÓPEZ-COLINA[b], MARÍA PELUFO[a]

*Dep. Construction. University of Oviedo
Campus de Viesques, 33203. Gijón, Spain
gayarre@uniovi.es

[a] ETSICCP. Polytechnic University of Valencia.
[b] Dep. Construction. University of Oviedo

Abstract

This article presents and develops a model for the behavior of steel fibers reinforced concrete (SFRC) for its use in plates elements. In order to carry out the present investigation, a series of laboratory tests were made for the mechanical characterization of SFRC. Additionally, a set of plates elements were tested in the laboratory of Construction Engineering at the Technical University of Valencia, with different fiber contents and load conditions. These plates elements were tested to their fracture, and the obtained results were verified experimentally with the implementation of the given model in a program of finite elements, where the tested plates were modelized. The obtained results show a satisfactory adjustment of the given model for its application in nonlinear calculation of plates elements made with steel fibers reinforced concrete.

Keywords: SFRC, ABAQUS, residual strength, strain, tensile strength, nonlinear calculation.

1. Introduction

The wide range of existing formulations and applications of steel fibers reinforced concrete make clear that it is not possible to adopt unique criteria for all types of fibers, all types of structural elements, nor all types and kinds of SFRC.

Traditionally, the compression tests in concrete have been used as a reference for their mechanical characteristics and as a parameter in the structural design of concrete elements. When steel fibers are added up to concrete, the compression strength does not experience a significant change, especially when the fiber content is the habitual one. Although this

parameter cannot represent the complete development of the mechanical characteristics of SFRC, it can also be used in this case to characterize its conventional strength in the design.

The presence of fibers in the concrete matrix causes the tensile stress – strain diagram (σ-ε) to be substantially altered. In concrete without fiber addition there is a practically elastic first stage, followed by a micro-cracking that leads quickly to a fragile failure of the material. The behavior is usually different with fibers, depending on their type and volume, as in Absi[1] or ACI [2]. The first stage is similar to concrete without fibers, almost linear; the second stage is developed by means of an increasing curve during which the concrete cracks and the fibers begin to tense up; and in the last stage, the stress is supported by fibers that tie the cracks. The fibers then, give a significant increase of the corresponding deformation to the maximum tensile stress applied and quite a smaller slope in the downward stage, as in Kosaka [3].

With respect to the elastic modulus with habitual values of fiber content (< 1%), significant modifications cannot be expected with respect to concretes without fiber content, as in Barros [4].

Hillerborg [5] [6] [7], shows that the cracking process in a specimen of SFRC can be characterized by the stress-crack opening curve, which can be obtained directly from a direct tensile test. It seems then, that this curve may be a good way to characterize the behavior of SFRC. Nevertheless, its determination is not simple and sophisticated test devices are required in order to allow a uniform load and controlled displacements during the specimen test. This fact justifies that different authors analyze this cracking process by means of its toughness and its corresponding indexes that characterize, not only the fracture energy but also the shape of the behavior curve of the SFRC as in Saldivar [8] or Wang [9] or Gettu [10].

The investigation took into account a theoretical approach to the model of behavior based on the state of the art of steel fibers reinforced concrete. Diverse tests were planned in order to determine the values associated to the theoretical proposed model. Additionally, several tests were made in square plates with the purpose of being able to compare experimentally the behavior of the proposed model and thus justifying the model's validity.

The purpose of the current investigation consists of studying the behavior of the steel fibers reinforced concrete in plates elements, where the tensile stress, associated or not to flexions, are vital in the design, and due to its thinness, it is difficult to achieve an adequate conventional reinforcement. The obtaining of the parameters that characterize the compression behavior of SFRC does not present significant discussion. Nevertheless, obtaining of the parameters that characterize the tensile behavior of SFRC is being widely discussed at the present time and it is in this point on which the present work of investigation is focused.

2. Experimental investigation.

An experimental program with two objectives was considered. Firstly, to characterize the mechanical behavior of the SFRC in order to establish the parameters that define the behavior model, and secondly, to make tests on elements such as square plates

1.20×1.20×0.06 m, with sufficient size to consider them as representative of a real construction.

These plates elements were tested under different load hypotheses and fiber content. The results of the tests were compared with the results of the numerical simulation and they will be explained as follows.

The fiber content and the load system were considered as variable within the investigation. The study used four different fiber contents and three different load systems. From each combination three plates were tested giving a total of 36 units. The fiber contents were 0, 50, 70 and 90 kg of fibers/m^3 of concrete and the load systems were:

(a) the specimen was leaned on two lines a meter apart, the load was introduced progressively and was made of two linear loads applied at 30 cm of the supports.

(b) the specimen was tested with four point loads forming a 40 cm centered square and it leaned on four points that formed a 1.00 m square.

(c) the specimen was tested with two point loads centered on the same line, separated 60 cm and it leaned on four points that formed a 1.00 m square.

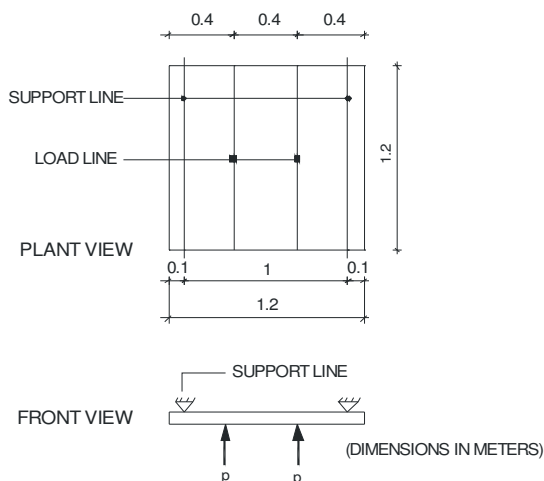The **figures 1, 2** and **3** show the different load systems.
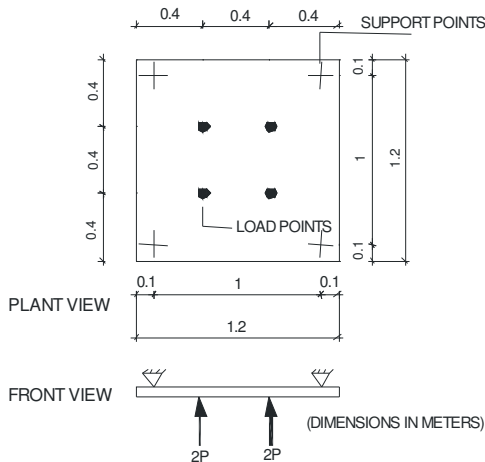

Figure 1: First load system.
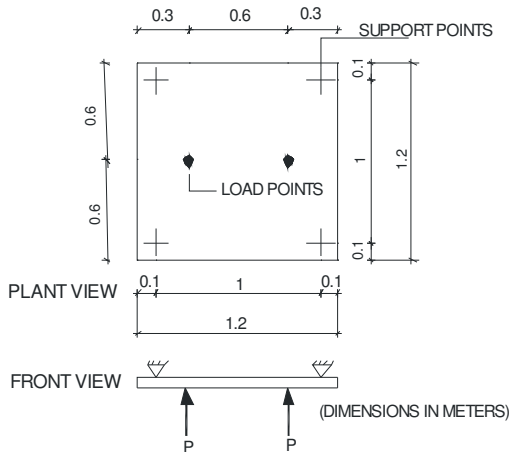
Figure 2: Second load system.

Figure 3: Third load system.

The used fibers were RC 80/35 BN, which are steel fibers of wire stretched in cold with ends conformed and glued in combs, DRAMIX brand. The concrete used in specimens was produced in the plant with initial conditions such as compression strength 25 MPa , fluid consistency and a specific grain size analysis. The conditions previous to the test were analyzed by mean of laboratory tests. The following tests were made to determine the concrete characteristics of the plates specimens:

• Slump value obtained by means of the Abrams cone following the Spanish standard UNE - 83313.

• Aggregate content and fiber content obtained by sieve washing No 4 following the Spanish standard 83512-1.

• Compression Strength, made on 15 x 30 cm cylindrical specimens following the Spanish standard UNE 83508. There were made six specimens for each fiber contents.

• Direct tensile in 11x30 cm cylindrical specimens with controlled speed of crack opening. The stress-crack opening curves were obtained up to 2 mm crack width. This process was made according to the one proposed by RILEM TC-162. For each fiber contents there were made eight specimens.

• Flexural tension test in prismatic specimens following the Spanish standard UNE 83510. For each fiber content six specimens were tested.

3. .Exposition of the proposed model

Figure 4 shows the proposed model that involves a tensile behavior diagram of SFRC made up by three simple stages, as in Domingo [11], [12]. The first stage corresponds to an elastic and linear behavior of SFRC before its cracking and it is defined by the tensile elastic modulus *E SFRC* - that fits in with the compression elastic modulus and the y axis corresponding to the value of the maximum tensile strength σ_t before the cracking, obtained indirectly by means of the flexural tensile test.
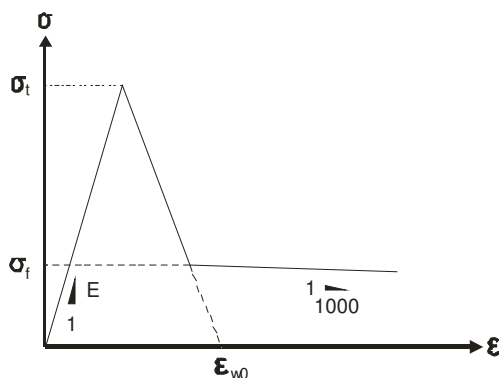

Figure 4: Proposed model for tensile behavior of the SFRC.

When the maximum stress is reached, the SFRC cracks and it is assumed a stage of falling stresses similar to a conventional concrete's one. This decrease, considering a stress-crack opening behavior diagram for concrete to which fibers have not been added, would fall until a crack opening of 0.02 mm. If this crack opening is related to its characteristic length, we will obtain the strain ε_{w0}, as in Crisfield [13]. The intersection of this straight line with its horizontal from the value of the tensile strength σ_f provides the end of the second stage and the beginning of a third one, from which the SFRC develops its ductile behavior, represented in the diagram by a basically horizontal straight line with a 0.1% slope. This residual strength σ_f is also obtained by means of the flexural tensile test.

For the justification of the proposed model we will analyze the behavior of a specimen of SFRC tested to flexural tension. We will distinguish two different situations in this test, one until cracking and another one after it. Let us suppose a behavior of the specimen tested under flexural tension as shown in **Figure 5**.
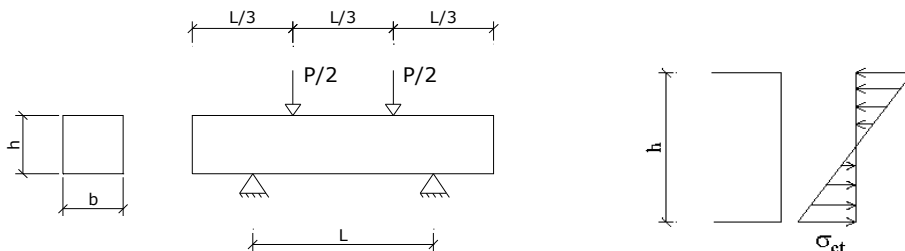
Figure 5 – Behavior of the central area in the specimen before cracking.

The bending moment in the central area at the moment of cracking is worth:

$$M = \frac{\sigma_{ct} \cdot b \cdot h^2}{6}$$

Where σ_{ct} is the tension developed by fibers at the most tensile edge.
On the other hand, the bending moment in the middle span is worth:

$$M = \frac{P \cdot l}{6}$$

From where the maximum value of the stress in the test is:

$$\sigma_{ct} = \frac{P \cdot l}{b \cdot h^2}$$

and according to the EHE [14], σ_t can be calculated as:

$$\sigma_t = 0,6 \cdot \sigma_{ct}$$

The section's behavior changes substantially when the specimen cracks. ACI [15], Dramix [16] and Vandewalle [17] propose different models of behavior currently, but their ultimate aim is the application of their model in linear elements but not in plates elements as in this case. This way, the proposed model starts with the hypothesis that the block of compressions can be practically reduced to only the superior fibers being compressed and the rest of the section having a rectangular uniform tension as shown **Figure 6**.
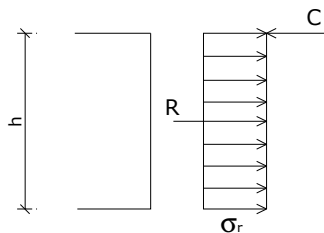
Figure 6 – Distribution of stresses in the section after cracking.

Therefore,

$$\sigma_f = \frac{PL}{3 \cdot b \cdot h^2}$$

As it is tried to analyze the average behavior of the specimen after cracking until a high level of deformation has considered a curve of answer simplified to flexural tension supposing a rigid-plastic behavior as shown in **Figure 7**.
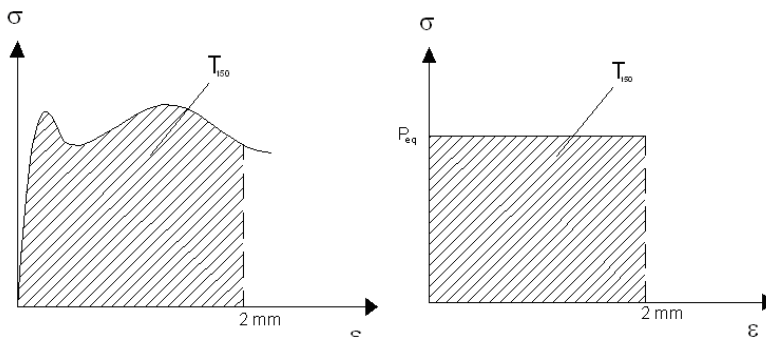

Figure 7 – Exposition of the behavior to flexural tension.

The process is reduced to calculate the equivalent load that would demand the same energy to reach the deflection of 2 mm (l/150). This energy can be calculated experimentally (T_{150}) and, therefore, the value of P_{eq} will be:

$$P_{eq} = \frac{1}{2} \cdot T_{150}$$

And the value of the cracking stress will be:

$$\sigma_f = \frac{P_{eq}L}{3 \cdot b \cdot h^2} = 1/3 f_{ct,eq,150}$$

4. Results.

Figure 8 shows the characterization results for different fiber contents. This table includes the theoretical and experimental fiber contents, the average aggregate content and the obtained slump.

Concrete	Theoretical content (kg/m^3)	Measured content (kg/m^3)	Aggregate (kg/m^3)	Slump (cm)
1	0	-	596	6
2	50	41.9	678	12
3	70	64.5	733	9
4	90	87.2	835	7

Figure 8 – SFRC Characterization.

Figure 9 summarizes the results of the compression tests and it also shows the concrete elastic modulus. In general, this table shows the same pattern behavior for each fiber contents and it also shows that an increase in the fiber contents produces a low increase in the compression strength. In addition, the values of standard deviation show that the behavior of the concrete is uniform.

Fibers (kg/m^3)	Compresive strength (MPa)	Standard deviation (MPa)	E (MPa)	Standard deviation (MPa)
0	25.58	0.79	26950	2720.4
50	19.76	2.17	25490	3425.1
70	23.57	1.9	28950	3098.6
90	26.59	0.87	28742	3702.4

Figure 9 – Compression tests results.

With respect to direct tensile tests, **figures 10 to 13** show the experimental measurements of the stress-crack opening curve. Additionally, **Figure 14** summarizes the previous curves where rectangle ABCD represents the crack energy by area unit. The toughness for 2 mm (T_2) was considered as the rectangle area up to a 2 mm width opening. The experimental results are summarized in **figure 15**, showing a good agreement between the proposed model and test results.
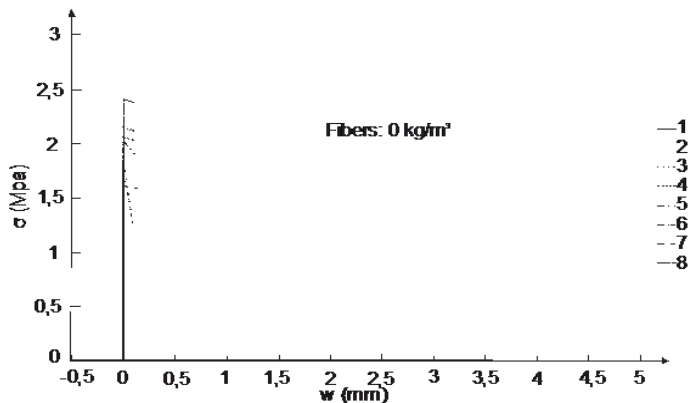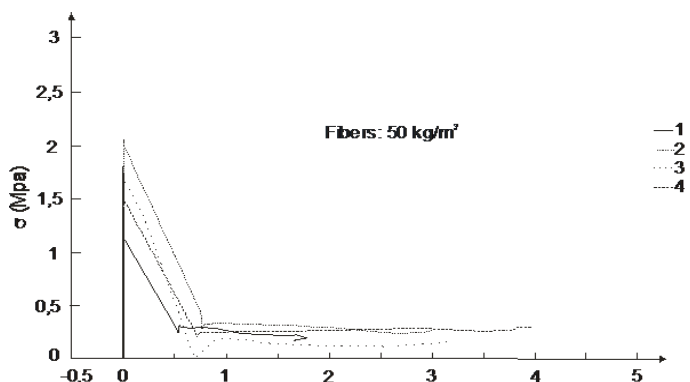
Figure 10 – Tensile test results - fibers: 0 kg/m^3.
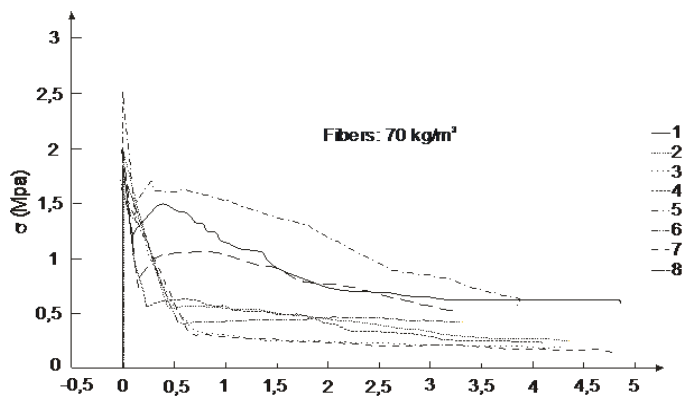

Figure 11 – Tensile test results - fibers: 50 kg/m^3.
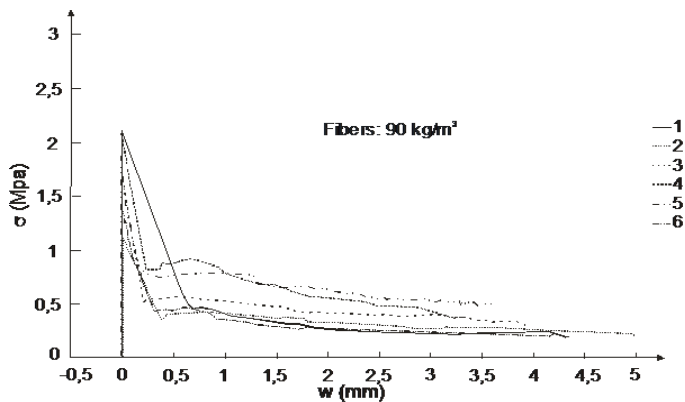

Figure 12 – Tensile test results - fibers: 70 kg/m^3.
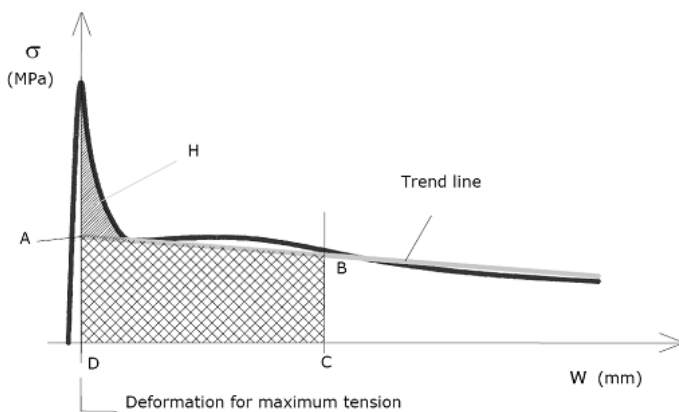
Figure 13 – Tensile test results - fibers: 90 kg/m^3.

Figure 14 – Stress-crack opening curve.

Fibers (kg/m^3)	σ_t (MPa)	Standard deviation (MPa)	T_2 (N/mm)	Standard deviation (N/mm)	$\sigma_{t,2}$ (MPa)
0	2,06	0,11	-	-	-
50	1,74	0,14	0,51	0,3	0,25
70	1,98	0,12	1,44	0,63	0,72
90	1,78	0,13	1,03	0,31	0,51

Figure 15 – Direct tensile tests results.

Characteristic values were abstracted from the flexion tests on prismatic specimens: P_f load at first crack, P_r ultimate load and the displacement energy which is the area under the diagram up to the l/300 deflection and l/150 span width, T_{300} (1 mm) and T_{150} (2 mm), respectively. **Figure 16** shows the results obtained by means of flexural tension tests. With these values, the flexural tension strength σ_{ct}, the residual strength corresponding to a l/150 $f_{ct,\ 150}$ deflection, the maximum tensile strength σ_t and the residual strength σ_f can be calculated.

Fibers (Kg/m^3)	Average value				Standard deviation			
	P_f (kN)	P_r (kN)	T_{300} (Nm)	T_{150} (N·m)	P_f (kN)	P_r (kN)	T_{300} (N·m)	T_{150} (N·m)
0	13.75	-	-	-	1.77	-	-	-
50	13.27	17.54	9.98	21.17	1.23	6.28	3.11	7.69
70	15.02	26.39	16.3	33.05	2.18	10.37	6.08	13.1
90	15.41	29.5	17.83	35.45	1.91	3.48	1.79	4.54

Figure 16 – Flexural tensile tests results.

According to the results of these last tests, the following simplifications were made: E value is the same for tension and compression, σ_t is related with the flexural tension strength in the following way $\sigma_t = 0.60\ \sigma_{ctb}$. The use of σ_{ct} was restricted due to the fact that the results were low in numerical value and dispersed. **Figure 17** shows the model parameters obtained through previous tests.

Fibers (kg/m^3)	E (MPa)	σ_t (MPa)	σ_f (MPa)	ε_0	ε_{w0}(mm)
0		2.47	-		
50	30000	2.39	1.06	1.5×10^{-4}	0.02
70		2.71	1.65		
90		2.77	1.77		

Figure 17 – Model parameters.

5. Implementation in a finite element model.

With the purpose of verifying analytically the proposed model and to study the behavior of SFRC plates, the model proposed was implemented in a finite element analysis program. The ABAQUS/Standard program was chosen for this implementation. This is an analysis program based on the Method of Finite Elements (MFE) that can deal with a great variety of problems in the engineering field and it is a powerful tool in the analysis of nonlinear, static or dynamic problems in mechanics.

First the stress-strain curve was introduced in the proposed model in the ABAQUS/Standard finite elements software. The first tests were made with the parameters

obtained experimentally in concrete with a 90 kg/m^3 fiber content and for the second load system. Two resolution systems of the problem were considered:

on one hand, by using Riks method and on the other hand, by imposing deformations. In both cases the problem was not solved by lack of convergence in the solution, but the resolution of the problem fails when it goes from the elastic behavior to the plastic one. The same process was repeated for the rest of fiber contents and load systems, reaching the same conclusion.

The previous experiment leads to consider a smoother transition between both behaviors. As an alternative solution it was considered to define the transition between both behaviors in a smooth way by rounding up the peak of the stress–strain curve. In the first place, the introduction of this curve would mean that the tensile fracture stress had to be placed at the end of the linear stage of the elastic behavior, as the software assumes that the behavior must be linear until this stress, not admitting any other type of behavior.

Secondly, as a consequence of the previous supposition, the final stage of the curve in the elastic behavior is transformed into a hardening curve after the cracking for deformations very near the corresponding tensile fracture stress, to fall later in a little bit smoother way than the model proposed initially. This exposition would be equivalent to admitting a stress increase after cracking, but it could be admitted as valid for a very small deformation area with the purpose of giving a better convergence in the problem resolution as long as it did not suppose a sensible increase in the global deformation energy.

Analyzing the previous experiment, a stress-strain curve was continued with only one linear stage in the elastic behavior. Also it was decided to smooth the first softening stage in plastification in a more explicit way, causing a smoother fall after cracking that will help a better convergence in the problem solution.

In the following **Figure 18** the final proposed model is presented and this is the one that was implemented in ABAQUS software.
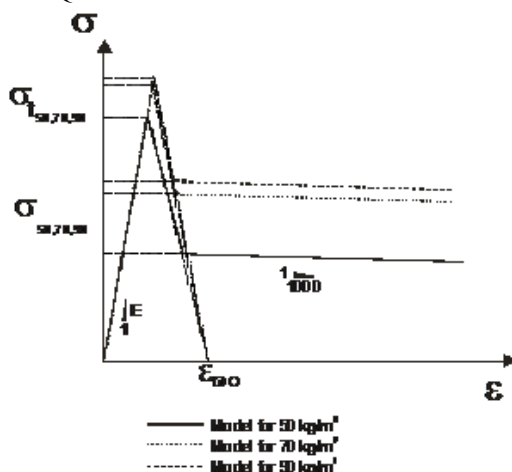
Figure 18 – Final proposed model.

6. Model verification.

The following **figures 19 to 22** show the most important tests results on plates specimens corresponding to load systems *b* and *c* for different fiber contents. The corresponding results for the finite element model are superposed in each figure. The total load in comparison with the deformation was presented until high levels of displacement.

These figures show a good agreement between the experimental model and the finite element model. The load process can be applied until high levels of displacement. The load systems *b* and *c* give good results and the load system *a* results show variability. This behavior is related to the capacity of stress redistribution in the load systems *b* and *c*. Cracks appear little concentrated but of greater dimension in low fiber contents, and in addition, there is a fast decrease after the load peak and the appearance of the first crack (fragile material). On the other hand, for fiber contents around 70 kg/m^3 the cracking showed an ampler pattern and a progressive behavior that indicates a more ductile behavior.
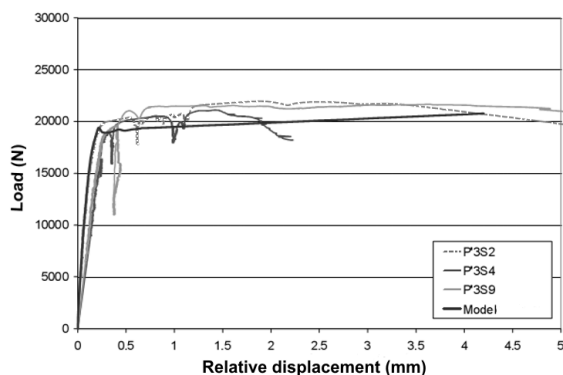

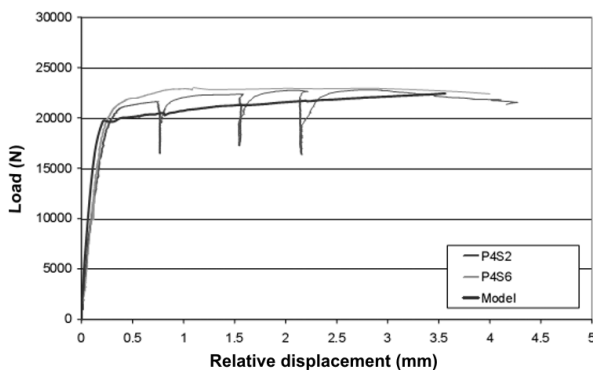Figure 19 – Load- relative displacements. 70 kg/m3 fibers load system *b*.

Figure 20 – Load- relative displacements. 90 kg/m^3 fibers load system *b*.
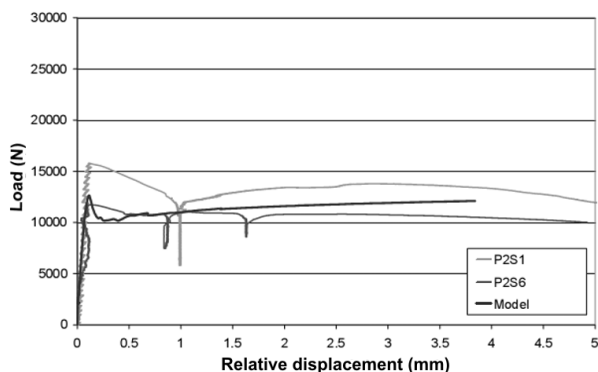
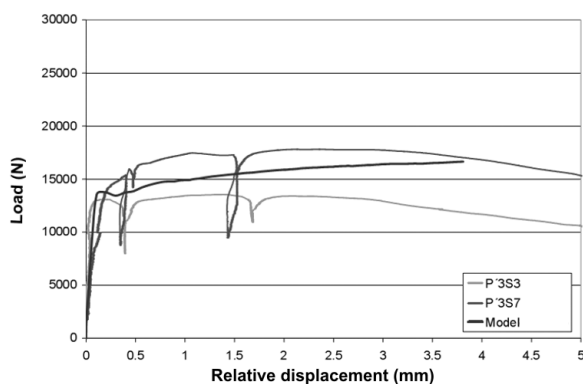Figure 21 – Load - relative displacements. 50 kg/m^3 fibers load system *c*.

Figure 22 – Load - relative displacements. 70 kg/m^3 fibers load system *c*.

7. Conclusions.

The finite elements model shows good correlation with respect to the experimental results.

The model is able to simulate the answer in the cracking process, involving a fast stress decrease and a stress increase after cracking.

The fiber addition does not represent a relevant improvement to the development of the compression strength of the concrete.

The behavior of concrete plates with steel fibers is different in relation to the load system. When the plates is loaded under flexion in two different directions, the redistribution of stresses is made easily and the behavior is more ductile. In the case of plates working at simple flexion, the answer is more fragile and the results of the different plates are more dispersed.

Additionally, when the fiber content is high and the load allows a redistribution of stresses, the theoretical proposed approach is quite good. For the case where the fiber content is low or the redistribution of stresses is not guaranteed, the theoretical answer continues adapting to the average behavior of the tested plates. Nevertheless, the greatest experimental dispersion provokes a bigger number of tests and a cautious analysis of the theoretical results.

8. References.

1. Absi, E; "Béton de fibres. Synthèse des études et recherches réalisées au CEBTP"; Annales de l'ITBTP; January 1994.

2. ACI Committee 544; "Measurements of properties of fiber reinforced concrete"; ACI Materials Journal, Vol. 85, N. 6, pp. 583 – 593; 1988.

3. Kosaka, Y.; Tanigawa, Y.; Hatanaka, S.; "Lateral confining stresses due to steel fibres in concrete under compression"; The International Journal of Cement Composites and Lighweight Concrete, Vol. 7, N. 2; May 1985.

4. Barros, J. A. O.; Figueiras, J. A.; "Flexural Behavior of SFRC: Testing and modeling"; Journal of materials in civil engineering, vol. 11, nº 4, pp. 331-339; 1999.

5. Hillerborg, A.; "Analysis of fracture by means of the fictitious crack model, particularly for fibre reinforced concrete"; The International Journal of Cement Composites, The construction Press Ltd., vol. 2, nº 4, pp. 177-184; 1980.

6. Hillerborg, A.; Hannat, D.J.; "Thoughness of fibre cement composites"; Composites, Vol. 13, pp.105-111; April 1982.

7. Hillerborg, A.; Modéer, M.; Peterson, P. E.; "Analysis of crack formation and crack growth by means of fracture mechanics and finite element"; Cement and Concrete Research, Vol. 6, No.6, pp. 773-781; Nov. 1976.

8. Saldivar, H.; "Flexural Toughness Characterization of Steel Fiber Reinforced Concrete. Study of Experimental Methodologies and Size Effects"; Doctoral Thesis; Directors: Ravindra Gettu, Antonio Aguado, Polythecnical University of Catalonia; October 1998.

9. Wang, Y.; Backer, S.; "Thoughness determination for fibre reinforced concrete"; The international journal of cement composites and lightweight concrete, Longman Group UK Ltd 1989, vol. 11, nº 1, pp. 11-19; USA; 1989.

10. Gettu, R.; Barragán, B.; Zalochi, R. F.; Martín, M. A.; Agulló, L.; "A comparative study of the toughness of steel fiber reinforced concrete in tension, flexure and shear"; Fibre-Reinforced Concretes (FRC) BEFIB' 2000, Proceedings of the Fifth International RILEM Symposium,; pp. 441 – 450; 2000.

11. Domingo, A.; Lázaro, C.; Serna, P.; "Use of steel fiber reinforced concrete in thin shell structures: evaluation of fiber performance through testing of shell specimens"; Computational methods; Athens, Greece; 2000.

12. Domingo, A.; Lázaro, C.; Serna, P.; "Using a postfailure stress-displacement material model for SFRC plates. Evaluation through testing of shell specimens"; International

symposium on Theory, Design and Realization of Shell and Spatial Structures, IASS, H. Kinieda; Nagoya, Japan; 2001.

13. Crisfield, M. A.; "Snap-through and snap-back response in concrete structures and the dangers of under-integration"; International Journal for numerical methods in engineering, John Wiley & Sons, Ltd., vol. 22, pp. 751-767; 1986.

14. EHE, Instrucción del hormigón estructural; Ministerio de Fomento; Spain; 1998.

15. ACI Commitee 544.4R-88 (Reapproved 1994); "Design Consideration for Steel Fiber Reinforced Concrete"; ACI Manual of concrete practice; 1999.

16. Dramix Guideline; "Design of concrete structures. Steel wire fiber reinforced concrete structures with or without ordinary reinforcement"; Infrastructuur in het leefmilieu, Departement Leefmilieu en infrastructuur, nº 4, pp. 226-239; 1995.

17. Vandewalle, L.; "Design method for steel fiber reinforced concrete proposed by RILEM TC 162-TDF"; Fiber-Reinforced Concrete (FRC). BEFIB' 2000, Proceedings of the Fifth International RILEM Symposium, Ed. by Rossi and G. Chanvillard, pp. 51-64; September 2000.